Published OnlineFirst March 31, 2009; DOI: 10.1158/1940-6207.CAPR-08-0211

ABT-510 Is an Effective Chemopreventive Agent in the Mouse 4-Nitroquinoline 1-Oxide Model of Oral Carcinogenesis

Rifat Hasina,[1] Leslie E. Martin,[1] Kristen Kasza,[2] Colleen L. Jones,[1] Asif Jalil[1] and Mark W. Lingen[1]

Abstract Despite numerous advances, the 5-year survival rate for head and neck squamous cell cancer (HNSCC) has remained largely unchanged. This poor outcome is due to several variables, including the development of multiple primary tumors. Therefore, it is essential to supplement early detection with preventive strategies. Using the 4-nitroquinoline 1-oxide (4-NQO) mouse model, we sought to define an appropriate dose and duration of administration that would predict the histologic timeline of HNSCC progression. Additionally, we sought to determine the timing of the onset of the angiogenic phenotype. Finally, using ABT-510 as a proof-of-principle drug, we tested the hypothesis that inhibitors of angiogenesis can slow/delay the development of HNSCC. We determined that 8 weeks of 100 μg/mL 4-NQO in the drinking water was the optimal dosage and duration to cause a sufficient incidence of hyperkeratoses, dysplasias, and HNSCC over a period of 32 weeks with minimal morbidity and mortality. Increased microvessel density and vascular endothelial growth factor expression in hyperkeratotic lesions provided evidence that the initiation of the angiogenic phenotype occurred before the development of dysplasia. Importantly, ABT-510 significantly decreased the overall incidence of HNSCC from 37.3% to 20.3% ($P = 0.021$) as well as the combined incidence of dysplasia and HNSCC from 82.7% to 50.6% ($P < 0.001$). These findings suggest that our refinement of the 4-NQO model allows for the investigation of the histologic, molecular, and biological alterations that occur during the premalignant phase of HNSCC. In addition, these data support the hypothesis that inhibitors of angiogenesis may be promising chemopreventive agents.

At current rates, approximately 400,000 cases of head and neck squamous cell cancer (HNSCC) will be diagnosed worldwide this year (1). Despite numerous advances in therapy, the long-term survival for these patients has remained largely unchanged. Several factors contribute to this poor outcome. First, oral cancer is often diagnosed in an advanced stage. The 5-year survival rate of early-stage oral cancer is approximately 80%, whereas the survival drops to 19% for late-stage disease (2). Second, the development of multiple primary tumors has a major effect on survival. The rate of second primary tumors in these patients has been reported to be 3% to 7% per year, higher than for any other malignancy (3). The observation of frequent second primary tumors in oral cancer led Slaughter et al. (4) to propose the concept of "field cancerization." This theory suggests that multiple individual primary tumors may develop independently in the upper aerodigestive tract as a result of years of chronic exposure to carcinogens. The occurrence of these new primary tumors can be particularly devastating for individuals whose initial lesions are small. Their 5-year survival rate for the first primary tumor is considerably better than patients with late-stage disease. However, second primary tumors are the most common cause of treatment failure and death among early-stage HNSCC patients (5). Therefore, it is insufficient treatment to address only the initial lesion. To improve the outcome of such patients, some form of chemopreventive treatment is essential.

Chemoprevention can be defined as the systemic use of natural or synthetic agents to reverse or halt the progression of premalignant lesions. Chemopreventive agents are being tested for their efficacy in the preclinical and clinical settings for several malignancies, including HNSCC (6). However, the initial promising responses have not been consistently reproduced and toxicity was often a significant issue. Therefore, more effective and better tolerated therapy is needed for premalignant oral disease.

Angiogenesis, the growth of new blood vessels from preexisting ones, is an essential phenotype in several physiologic and pathologic processes, including growth and development, wound healing, reproduction, arthritis, and tumor formation

Authors' Affiliations: Departments of [1]Pathology, Medicine, and Radiation and Cellular Oncology and [2]Health Studies, The University of Chicago, Chicago, Illinois

Received 11/13/08; revised 2/7/09; accepted 3/4/09; published OnlineFirst 3/31/09.

Grant support: Abbott Laboratories and NIH grant DE012322.

The costs of publication of this article were defrayed in part by the payment of page charges. This article must therefore be hereby marked *advertisement* in accordance with 18 U.S.C. Section 1734 solely to indicate this fact.

Requests for reprints: Mark W. Lingen, Department of Pathology, The University of Chicago, 5841 South Maryland Avenue, MC 6101, Chicago, IL 60637. Phone: 773-702-5548; Fax: 773-702-9903; E-mail: mark.lingen@uchospitals.edu.

doi:10.1158/1940-6207.CAPR-08-0211

Published OnlineFirst March 31, 2009; DOI: 10.1158/1940-6207.CAPR-08-0211

(7). Whether active neovascularization occurs is dependent on the relative concentrations of inducers and inhibitors of angiogenesis present in a given tissue microenvironment. Therefore, the inhibition of tumor-associated angiogenesis, using natural or synthetic inhibitors of angiogenesis, is an attractive target for therapy that has been gaining traction in the field of oncology. Like all solid tumors, HNSCCs must develop multiple direct and indirect ways to induce angiogenesis. Importantly, the expression of the angiogenic phenotype is one of the first recognizable phenotypic changes observed in both experimental models as well as in human HNSCC (8–11), suggesting that inhibitors of angiogenesis may also hold promise as chemopreventive agents. In addition to their main biological/molecular effects, some of the drugs currently under investigation in the chemopreventive setting have potential antiangiogenic activity. However, to date, no pure inhibitors of angiogenesis have been tested for their ability to act as chemopreventive agents in HNSCC.

Animal models that faithfully recapitulate the human condition are critical to further our understanding of the molecular, biological, and clinical aspects of various diseases, including cancer. The hamster buccal pouch and the rat tongue models of oral carcinogenesis are well-established surrogate models for the human condition. However, although the hamster buccal pouch and rat tongue models have been extensively investigated, they have several limitations, resulting in the recent development of mouse oral cancer models that have several advantages (12–18). In particular, mouse models enable the development and testing of new approaches to prevention and treatment, identification of early diagnostic markers, and an understanding of the biology and genetics of tumor initiation, promotion, and progression in an animal model whose genome is most similar to humans (19–22). Although the 4-nitroquinoline 1-oxide (4-NQO) mouse model of oral carcinogenesis has gained increased attention as an alternative model, several parameters require further investigation. For example, although various treatment protocols have been described, the optimal administration, timing, and dosage of 4-NQO required to develop lesions that clinically mimic the human condition (singular or synchronous neoplasms) have not been fully established. In addition, a detailed and systematic investigation of the histologic changes during progression in the 4-NQO mouse model before the development of HNSCC has not been done. Finally, the timing and mechanisms of the development of various tumor-related phenotypes have not been determined in this model. Each of these issues is of critical importance and must be addressed to determine how closely this model system mimics the human condition such that it can be used effectively for future preclinical studies.

Therefore, the purpose of this work was 4-fold. First, we sought to establish a dosage and treatment schedule that resulted in the development of singular or occasionally synchronous HNSCC rather than innumerable lesions throughout the oral cavity over a protracted period of time. Second, we established a predictable timeline for the histologic progression of mucosal lesions in mice treated with 4-NQO. Third, we sought to clarify when the expression of the angiogenic phenotype can be first observed in this model. Finally, ABT-510, a mimetic peptide of thrombospondin-1 (Fig. 1; refs. 23, 24), was administered to 4-NQO–treated mice as a proof of principle to test the hypothesis that inhibitors of angiogenesis can be successfully used as chemopreventive agents for HNSCC.

Materials and Methods

Administration of 4-NQO

Two hundred thirty male CBA mice, 6 to 8 wk of age, were purchased from The Jackson Laboratory and housed in the Animal Resource Facility under controlled conditions and fed normal diet and autoclaved water. All animal procedures were carried out in accordance with Institutional Animal Care and Use Committee approved protocols. Mice were administered 4-NQO in their drinking water on a continuous basis at the required dose for the required duration. 4-NQO powder (Sigma) was first dissolved in DMSO at 50 mg/mL as a stock solution and stored at −20°C until used. On the days of 4-NQO administration, the stock solution was dissolved in propylene glycol (Sigma) and added to the drinking water bottles containing autoclaved tap water to obtain a final concentration of either 50 or 100 μg/mL. A fresh batch of water was prepared every week for each of the 8 or 16 wk of carcinogenic treatment. Normal autoclaved drinking water was resumed at the end of this period. Control mice not receiving 4-NQO were given water containing vehicle only.

Treatment with ABT-510

ABT-510, a synthetic peptide that mimics the antiangiogenic activity of the naturally occurring protein thrombospondin-1, was provided by Abbott Laboratories. The peptide was dissolved in sterile

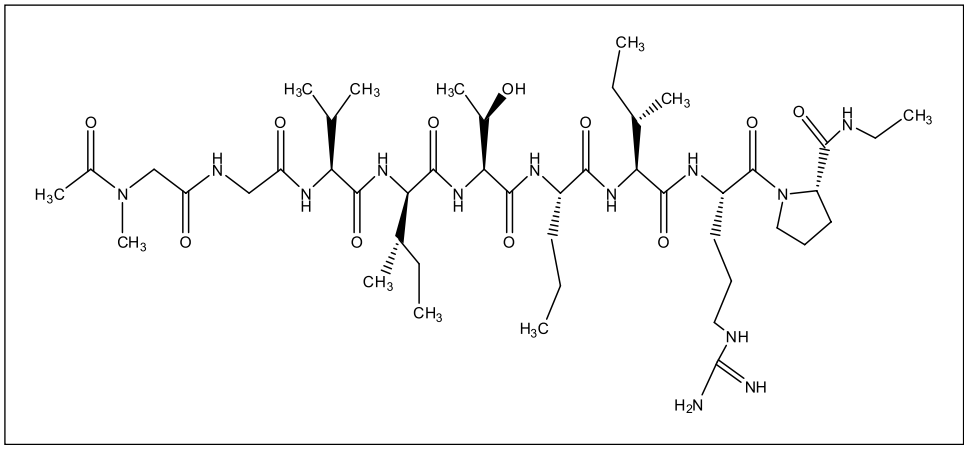

Fig. 1. Chemical structure of ABT-510. ABT-510 is a nonapeptide derived from the antiangiogenic fragment of the second type 1 repeat of thrombospondin-1. The key structures in the synthesis and the chemical structure from which this figure was derived can be found in the original publication by Haviv et al. (23).

Published OnlineFirst March 31, 2009; DOI: 10.1158/1940-6207.CAPR-08-0211

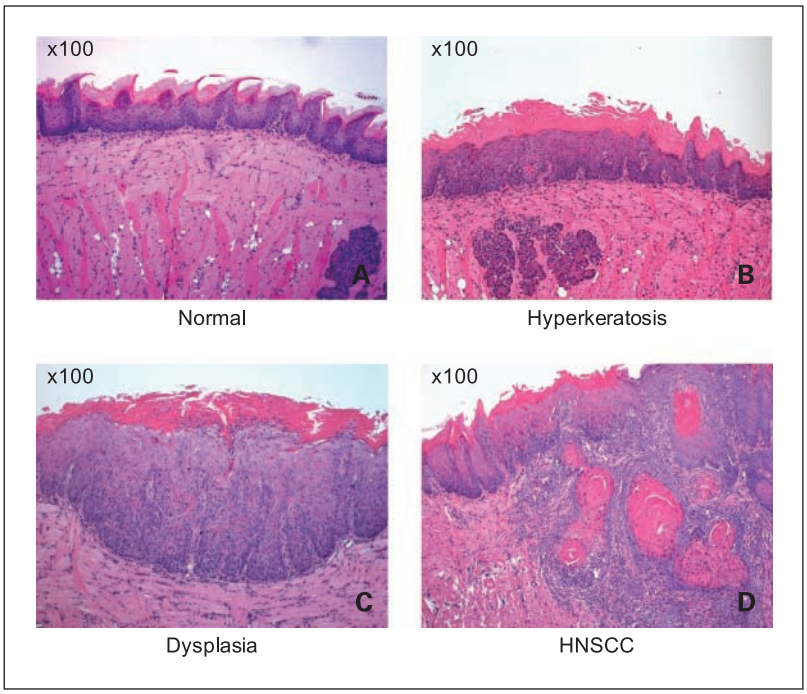

Fig. 2. Histopathology of 4-NQO–induced oral lesions in the mouse tongue. Photomicrographs show the histopathologic progression in this model system: histologically normal (control; *A*), hyperkeratosis (*B*), epithelial dysplasia (*C*), and squamous cell carcinoma (*D*).

5% dextrose, immediately filter sterilized, and stored at 4°C. Mice receiving ABT-510 treatment were given a daily i.p. injection of 50 mg/kg body weight for the required duration of 4, 8, 12, 16, 20, or 24 wk. The route of administration and dosage given was determined based on previously published studies (24–29).

Histologic examination

Mice were sacrificed in accordance with Institutional Animal Care and Use Committee recommendations. Specifically, cervical dislocation was done after anesthesia by i.p. injection of xylazine and ketamine. Immediately following death, the tongues were excised, longitudinally bisected, and processed in 10% buffered formalin and embedded in paraffin. Fifty 5-μm sections from each specimen were then cut and the 1st, 10th, 20th, 30th, 40th, and 50th slides were stained with H&E for histopathologic analysis. Histologic diagnoses were rendered using established criteria. Hyperkeratoses were characterized by a thickened keratinized layer, with or without a thickened spinous layer (acanthosis), and an absence of nuclear or cellular atypia. Dysplasias were characterized as lesions that showed various histopathologic alterations, including enlarged nuclei and cells, large and/or prominent nucleoli, increased nuclear to cytoplasmic ratio, hyperchromatic nuclei, dyskeratosis, increased and/or abnormal mitotic figures, bulbous or teardrop-shaped rete ridges, loss of polarity, and loss of typical epithelial cell cohesiveness. Because of the subjective nature of grading of epithelial dysplasia and its limited ability to predict biological progression (30, 31), we chose to not assign descriptive adjectives of "severity" to the dysplastic lesions. Rather, we grouped all lesions showing cytologic atypia but lacking evidence of invasion into the single category of dysplasia. HNSCCs were characterized by lesions that showed frank invasion into the underlying connective tissue stroma.

Immunohistochemistry

Antigen retrieval was achieved on deparaffinized sections and endogenous peroxidase activity was quenched in 3% hydrogen peroxide and blocked in milk peroxidase. For vascular endothelial growth factor (VEGF) detection, slides were treated in ET buffer in a decloaking chamber and mouse primary antibody (Santa Cruz Biotechnology) was applied at 1:50 dilution in PBS for 1 h at room temperature. Antibody binding was visualized with anti-mouse polymer-labeled horseradish peroxidase–bound secondary reagent (EnVision+, DAKO). CD31 antigen retrieval was done using the Dako Target Retrieval System (pH 9.0) in a decloaking chamber. The primary antibody PECAM (Santa Cruz Biotechnology) was applied at 1:200 dilution in PBS for 1 h at room temperature. Antibody binding was visualized using the LSAB kit (DAKO). For determination of cell proliferation, sections were treated in ET buffer using decloaking chamber, incubating at 1:300 dilution using a Ki-67 antibody (NeoMarkers) for 1 h at room temperature. This was followed by anti-rabbit polymer-labeled horseradish peroxidase–bound secondary reagent (EnVision+). All three immunohistochemistry stains were developed with 3,3′-diaminobenzidine chromogen and counterstained with hematoxylin. Corresponding negative control experiments were done by omitting the incubation step with the primary antibody.

Scoring of immunohistochemistry

A combined scoring method that accounts for intensity of staining as well as percentage of cells stained was used for the evaluation of VEGF as previously described (32). Strong, moderate, weak, and negative staining intensities were scored as 3, 2, 1, and 0, respectively. For each of the intensity scores, the percentage of cells that stained at that level was estimated visually. The resulting combined score consisted of the sum of the percentage of stained cells multiplied by the intensity scores. For example, a case with 10% weak staining, 10% moderate staining, and 80% strong staining would be assigned a score of 270 ($10 \times 1 + 10 \times 2 + 80 \times 3 = 270$) out of a possible score of 300. The determination of microvessel density (MVD) using CD31 as a marker was done as previously described (33). Briefly, using low-power magnification, the region containing the most intense area of tumor neovascularization was chosen for counting in each of the tumors. For the normal control tissue, MVD was determined by finding the most intense area of neovascularization directly below the overlying mucosa. Individual microvessels were counted using a 100× field (10× objective lens and 10× ocular lens). Any brown staining endothelial cells that were clearly separate in appearance were counted as individual vessels. Ten random fields within this hotspot area were viewed and counted at 100×. Results were expressed as the total number of microvessels observed in the "hotspot" region of each individual tumor. For Ki-67, the labeling indices were determined by randomly analyzing at least 500 nuclei in 10 high-powered fields (×400 magnification) for

Published OnlineFirst March 31, 2009; DOI: 10.1158/1940-6207.CAPR-08-0211

each tissue section. Labeling indices were expressed as a percentage of the total number of cells.

Data analysis

For comparison of immunohistochemical scores across groups, ANOVA was done. A transformation of the data (square root or natural log) was used, as needed, to stabilize the variance across groups. If a significant overall difference was found by ANOVA, then pairwise comparisons were done with a Bonferroni adjustment for multiple comparisons. A test for trend was also done using ANOVA with the appropriate linear contrasts, and these results were confirmed using a nonparametric trend test as described by Cuzick (34). For comparison of ABT-510 treatment groups, Fisher's exact test was done by collapsing data across the six sacrifice times. All analyses were done using Stata version 10 (StataCorp).

Results

Histopathologic progression of 4-NQO–treated mice

Articles describing the mouse 4-NQO model have typically reported the incidence of dysplasia and/or cancer at the end of the prescribed treatment protocols. However, these articles have not systematically characterized the sequential timing of histologic atypia development after carcinogen treatment over a protracted period of time. This is an important aspect of the model because a more thorough understanding of the histologic and molecular progression in this system is required if it is to be used to model oral premalignancy as well as preclinical chemoprevention studies. To carefully characterize the development of the histopathologic changes in this model, a series of pilot studies were done to identify the optimal carcinogen dosage and duration of exposure required to develop a predictable time line of progression. The animals were sacrificed at planned intervals after completion of carcinogen treatment, and their tongues were excised and examined histologically. No histopathologic changes were noted in the tongue mucosa from the control mice (Fig. 2A). Mice were treated with 50 μg/mL 4-NQO for 8 weeks (pilot study A) and 16 weeks (pilot study B). They were subsequently randomly assigned to groups and sacrificed at 4, 8, 12, and 24 weeks after 4-NQO treatment. From the initial 20 animals in pilot study A (50 μg/mL for 8 weeks), 4 mice died during treatment from undetermined causes. However, no subsequent deaths were observed in study A. At week 4 (n = 4), 75% of the tongues showed hyperkeratotic lesions, whereas 25% contained dysplasia. In the week 8 mice (n = 4), 25% had hyperkeratosis, 25% had dysplasia, and 50% had carcinoma. At 12 weeks (n = 4), 75% contained dysplasia and 25% had squamous cell carcinoma. Finally, by 24 weeks (n = 4), 25% showed dysplasia and 75% contained squamous cell carcinoma. Pilot study B (50 μg/mL for 16 weeks) was terminated early because of an excessive number of deaths. Of the initial mice, 40% (8 of 20) died either during carcinogen treatment or within 6 weeks after the completion of the carcinogen treatment. In pilot studies C and D, mice were treated with 100 μg/mL 4-NQO for either 8 weeks (pilot study C) or 16 weeks (pilot study D). In pilot study C (100 μg/mL for 8 weeks), there were no deaths during the study. At week 4 (n = 5), 100% of animals showed hyperkeratotic lesions (Fig. 2B). At week 8 (n = 5), 60% showed hyperkeratosis and 40% contained epithelial dysplasia (Fig. 2C). By 12 weeks (n = 5), 100% of animals had dysplasia. Finally, at week 24 (n = 5), 40% had dysplasia and 60% showed squamous cell carcinoma (Fig. 2D). Similar to pilot study B, unacceptable mortality rates were observed in pilot study D after animals were treated with 100 μg/mL for 16 weeks, resulting in the premature termination of this arm of the study as well.

Although this was a relatively small sample size, these results showed that a sequential histologic progression could be observed using this type of carcinogenic induction protocol. It further suggested that the majority of the dysplastic and cancerous lesion were likely to be found starting at 12 weeks after carcinogen treatment. Therefore, to expand on the pilot studies, a cohort of 55 additional mice was treated with 100 μg/mL 4-NQO for 8 weeks and tongues were subsequently harvested at weeks 16, 20, and 24. At week 16 (n = 20), 15% contained hyperkeratosis, 55% had dysplasia, and 30% showed squamous cell carcinoma. At 20 weeks (n = 15), 13% had hyperkeratosis, 60% contained dysplasia, and 23% showed squamous cell carcinoma. By 24 weeks after carcinogen treatment (n = 20), 25% of specimens contained dysplasia and 75% of the tissues showed squamous cell carcinoma. Collectively, the data for the 100 μg/mL 4-NQO administered for 8 weeks show a reproducible timeline of histologic progression. Specifically, the data show that hyperkeratotic

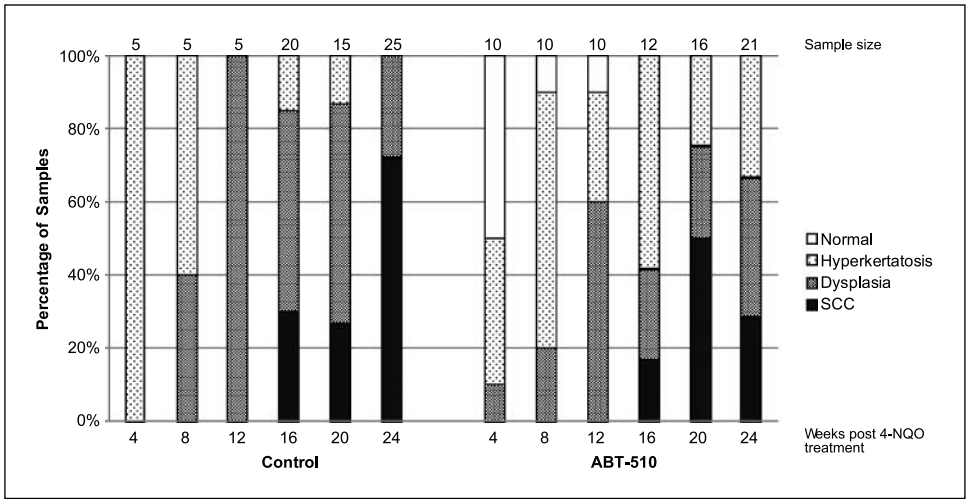

Fig. 3. Incidence of each histologic diagnosis of control and ABT-510 treatment groups at each sacrifice time. The number located at the top of each bar indicates the total sample size of each group. ABT-510 significantly decreased the incidence of HNSCC from 37.3% to 20.3% (P = 0.021) as well as the combined incidence of dysplasia and HNSCC from 82.7% to 50.6% (P < 0.001).

Published OnlineFirst March 31, 2009; DOI: 10.1158/1940-6207.CAPR-08-0211

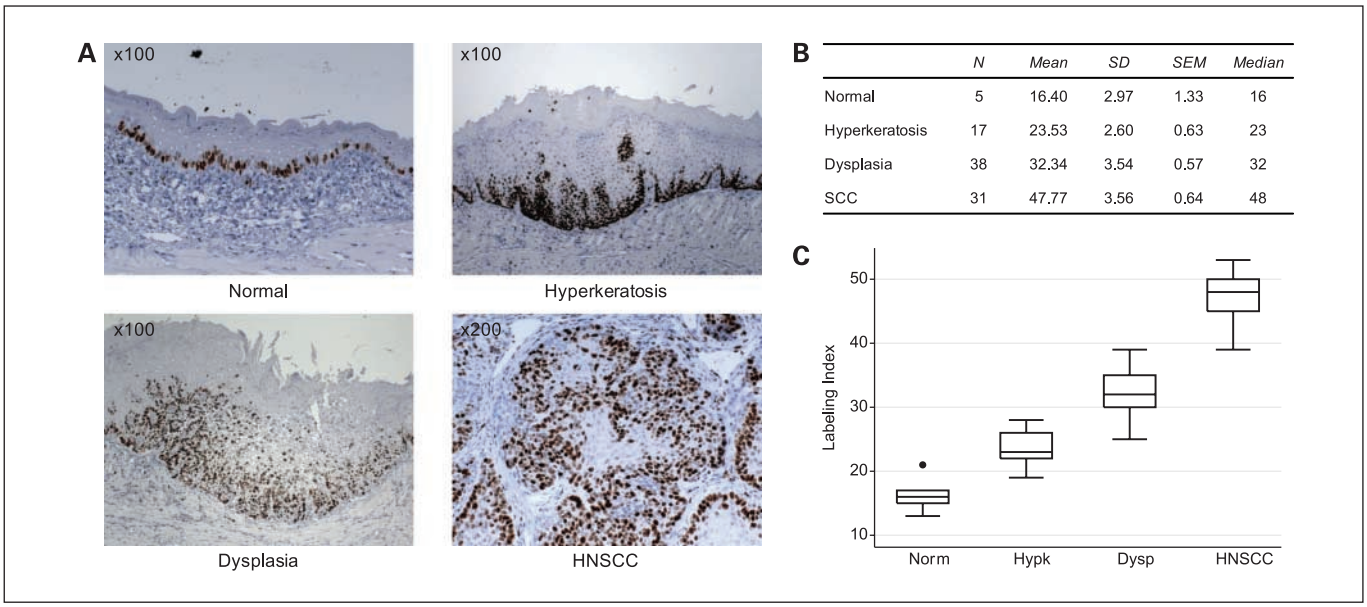

Fig. 4. Immunohistochemical staining of Ki-67 in the 4-NQO mouse model of HNSCC. *A*, tissue sections containing areas of normal, hyperkeratosis, dysplasia, and squamous cell carcinoma immunohistochemically stained for Ki-67 and labeling indices were quantified (*B* and *C*). Ki-67 labeling indices in the specimens containing hyperkeratosis, dysplasia, and HNSCC were all significantly greater when compared with the normal mucosa ($P < 0.001$).

lesions predominate at weeks 4 and 8, dysplasias are the most common diagnosis at weeks 12, 16, and 20, and carcinoma is the predominant histologic finding at week 24 (Fig. 3).

Ki-67 Expression during histologic progression in 4-NQO–treated mice

Expression of Ki-67, a nuclear proliferation-associated antigen that is specific for cells in the active phases of the cell cycle, was determined via immunohistochemistry to quantify the relative proliferative rates of normal, hyperkeratotic, dysplastic, and malignant mouse tongue mucosa. Cells positive for Ki-67 expression showed distinct nuclear staining. In normal mucosa, Ki-67 expression was limited to basilar and occasional parabasilar cells (Fig. 4A), whereas greater suprabasilar labeling was observed with increasing histologic atypia (Fig. 4A). There was a statistically significant difference ($P < 0.001$ by ANOVA) in labeling indices when normal epithelium (mean ± SD: 16.4 ± 3.0) was compared with hyperplasia (23.5 ± 2.6), dysplasia (32.3 ± 3.5), and squamous cell carcinoma (47.8 ± 3.6). Subsequent pairwise comparisons indicated that each group was significantly different from all other groups (Bonferroni adjusted $P < 0.001$ in all cases). Additionally, there was evidence for an increasing linear trend in Ki-67 levels across the four ordered groups (P for trend < 0.001; Fig. 4B and C).

Increased MVD occurs before histologic atypia in 4-NQO–treated mice

The induction of blood vessel growth is an early phenotypic change in both human HNSCC as well as in the hamster buccal pouch and rat tongue models of oral carcinogenesis (8–11). To determine the timing of the expression of the angiogenic phenotype in the 4-NQO mouse model, we did immunohistochemistry for CD31 to quantify MVD as a surrogate for *in vivo* angiogenesis activity. The connective tissue stroma adjacent to the mouse tongue epithelium from untreated control mice ($n = 5$) contained only occasional capillaries that were relatively evenly dispersed throughout the connective tissue stroma (Fig. 5A). However, the number and distribution of microvessels at the mucosal/connective tissue interface increased in the hyperplastic, dysplastic, and malignant mucosa (Fig. 5A). With increasing histologic atypia, the vessels were more densely packed directly adjacent to the basal cell layer. Quantification of MVD during histologic progression revealed a statistically significant difference ($P < 0.001$ by ANOVA) in CD31 scores when normal epithelium (mean ± SD: 23.2 ± 4.3) was compared with hyperplasia (90.2 ± 6.7), dysplasia (191.6 ± 10.6), and squamous cell carcinoma (309.3 ± 17.9). Pairwise comparisons indicated that each group was significantly different from all other groups (Bonferroni adjusted $P < 0.001$ in all cases). Furthermore, there was a significant linear trend in CD31 levels across the four naturally ordered groups (i.e., increasing CD31 levels with increasing disease severity; P for trend < 0.001; Fig. 5B and C).

Expression of VEGF during the histologic progression in 4-NQO–treated mice

Like all solid tumors, HNSCC must develop direct and indirect mechanisms to induce the production of new blood vessels. Several dozen candidate angiogenic molecules are produced by oral keratinocytes, and VEGF is an important angiogenic factor in both physiologic and pathologic settings, including HNSCC (35). Therefore, we did immunohistochemistry for VEGF to quantify its expression at various stages of histologic progression in the mouse 4-NQO model. Expression of VEGF by tongue keratinocytes from untreated control mice ($n = 5$) was rare and limited to the basilar and parabasilar cells (Fig. 6A). In addition, occasional stromal cells as well as endothelial lined vascular channels stained positively. The intensity of VEGF expression as well as the overall expression

Published OnlineFirst March 31, 2009; DOI: 10.1158/1940-6207.CAPR-08-0211

of the cytokine by various keratinocytes present in the different layers of the epithelium increased in the hyperplastic, dysplastic, and malignant mucosa (Fig. 6A). Quantification of VEGF expression among histologic stages revealed a statistically significant difference ($P < 0.001$ by ANOVA) when normal epithelium (mean ± SD: 17.0 ± 5.7) was compared with hyperplasia (70.6 ± 14.0), dysplasia (144.9 ± 35.4), and squamous cell carcinoma (237.6 ± 41.4). Each group was significantly different from all other groups (Bonferroni adjusted $P < 0.001$ in all cases). Most importantly, there also was evidence for an increasing linear trend in VEGF levels with disease progression (P for trend < 0.001; Fig. 6B and C).

Effects of ABT-510 administration in 4-NQO–treated mice

The expression of the angiogenic phenotype is one of the first recognizable phenotypic changes observed in both experimental models as well as in human HNSCC (8–11), suggesting that inhibitors of angiogenesis may also hold promise as chemopreventive agents. However, to date, no pure inhibitors of angiogenesis have been tested for their ability to act as chemopreventive agents in HNSCC. Therefore, using ABT-510 as a proof-of-principle drug, we tested the hypothesis that inhibitors of angiogenesis can be used as chemopreventive agents in the realm of HNSCC. Based on our findings described above, mice were administered 4-NQO (100 μg/mL) in their drinking water for 8 weeks. At the completion of this initiation phase, the mice were returned to normal water and given daily i.p. injections of ABT-510 (50 mg/kg/d) and sacrificed at regular intervals over the next 24 weeks. During the 24-week chemopreventive period, no significant differences in food or fluid consumption among the groups were observed. Similarly, there was no difference in body weight or activity between the control and the treatment group mice (data not shown). Data for the incidence of tongue lesions are shown in Fig. 3. At week 4 ($n = 10$), 50% of the tongues were histologically normal, 40% contained hyperkeratosis, and 10% had dysplasia. At week 8 ($n = 10$), 10% were normal, 70% contained hyperkeratosis, and 20% showed dysplasia. By week 12 ($n = 10$), 10% were normal, 30% contained hyperkeratosis, and 60% had dysplasia. At week 16 ($n = 12$), 58% had hyperkeratosis, 25% had dysplasia, and 17% showed carcinoma. Progressing to week 20 ($n = 16$), 25% had hyperkeratosis, 25% had dysplasia, and 50% showed carcinoma. Finally, at week 24 ($n = 21$), 33% had hyperkeratosis, 38% had dysplasia, and 29% showed carcinoma. With respect to overall incidence of cancer, a 46% reduction in HNSCC was observed, with the 4-NQO group having an incidence rate of 37.3% and the ABT-510 treatment group having an incidence of 20.3% ($P = 0.021$). In addition, the combined incidence of dysplasia and HNSCC was 82.7% in the 4-NQO control group and 50.6% in the ABT-510 treatment group. This difference was highly statistically significant ($P < 0.001$).

Discussion

Animal models of HNSCC have traditionally used either 7,12-dimethylbenz(*a*)anthracene or 4-NQO as the carcinogenic agent. The induction of HNSCC using 4-NQO has been achieved in several different rodent species, including mice, hamsters, and rats, and has been generally found to be preferable for several reasons. First, in contrast to the topical application of 7,12-dimethylbenz(*a*)anthracene, 4-NQO can be delivered via the drinking water, thereby making the outcomes more predictable. Second, the molecular alterations induced in mouse mucosa by 4-NQO closely mimic the human disease. For example, similar to the human condition, epidermal growth factor receptors are overexpressed in this model (36). Similar to humans, altered expression of p53 as well as mutation of p53 have been shown in 4-NQO models (37). In addition, 4-NQO induces activating point mutations in the H-ras oncogenes (38). Although H-ras mutations are infrequent events in U.S. HNSCC (39), they are common in the

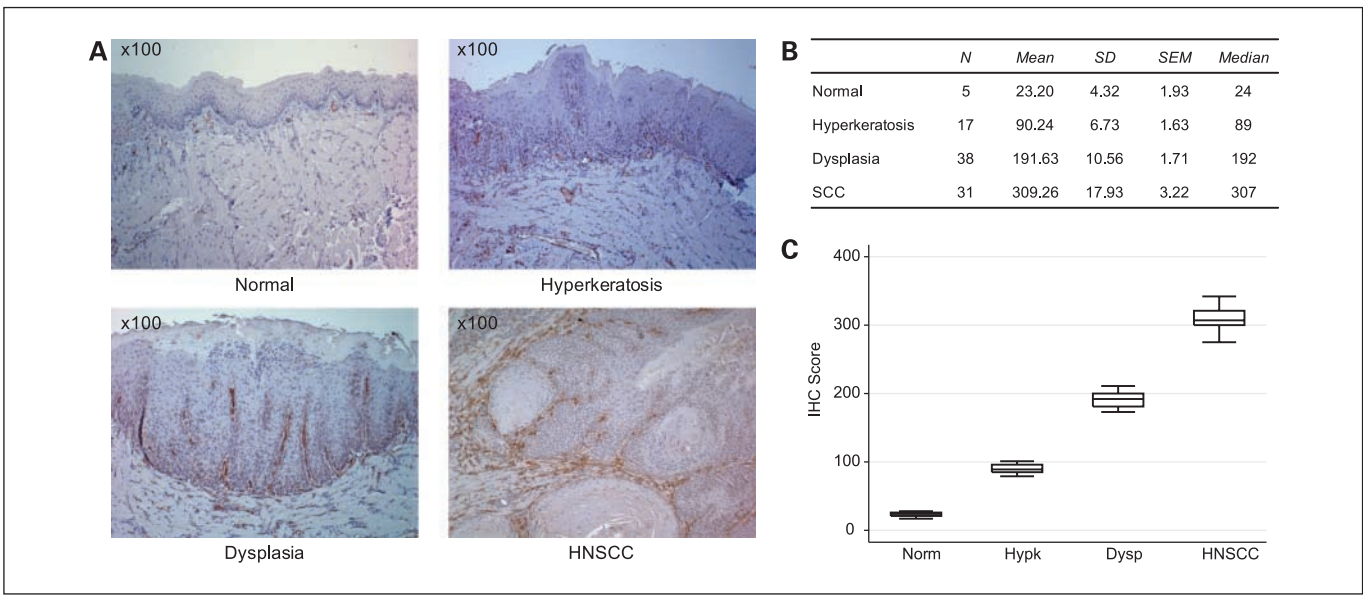

	N	Mean	SD	SEM	Median
Normal	5	23.20	4.32	1.93	24
Hyperkeratosis	17	90.24	6.73	1.63	89
Dysplasia	38	191.63	10.56	1.71	192
SCC	31	309.26	17.93	3.22	307

Fig. 5. Expression of the angiogenic phenotype in the 4-NQO mouse model of HNSCC. *A*, tissue sections containing areas of normal, hyperkeratosis, dysplasia, and squamous cell carcinoma immunohistochemically stained for CD31 and MVD was quantified (*B* and *C*). MVD in the specimens containing hyperkeratosis, dysplasia, and HNSCC was all significantly greater when compared with the normal mucosa ($P < 0.001$).

Published OnlineFirst March 31, 2009; DOI: 10.1158/1940-6207.CAPR-08-0211

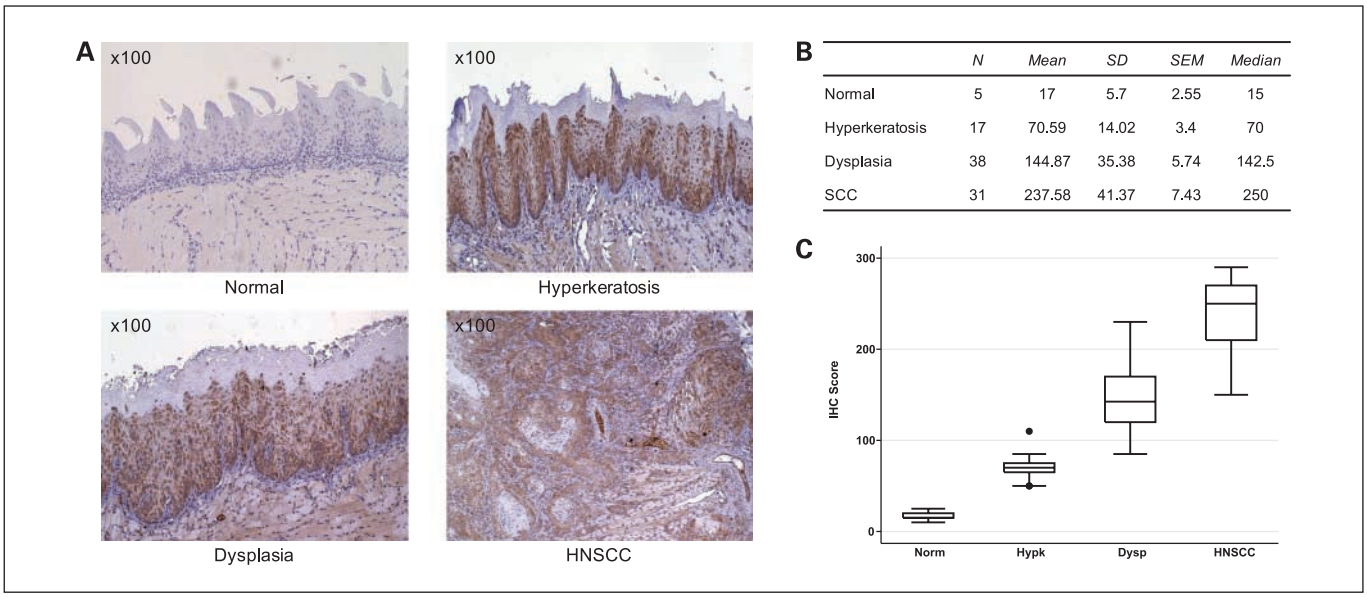

	N	Mean	SD	SEM	Median
Normal	5	17	5.7	2.55	15
Hyperkeratosis	17	70.59	14.02	3.4	70
Dysplasia	38	144.87	35.38	5.74	142.5
SCC	31	237.58	41.37	7.43	250

Fig. 6. Expression of VEGF in the 4-NQO mouse model of HNSCC. *A*, tissue sections containing representative areas of normal, hyperkeratosis, dysplasia, and squamous cell carcinoma immunohistochemically stained for VEGF and expression levels were quantified (*B* and *C*). Expression of VEGF in the specimens containing hyperkeratosis, dysplasia, and HNSCC was significantly greater when compared with normal mucosa ($P < 0.001$).

rest of the world (40). Therefore, because the majority of the 400,000 cases of HNSCC are outside of the United States/Europe and may therefore harbor H-ras mutations (in conjunction with epidermal growth factor receptor and p53 alterations), we believe that this is an excellent model from an experimental, histologic, and molecular perspective. Finally, 4-NQO–induced lesions develop in the absence of nonspecific inflammatory changes. This is a critical point because substances such as 7,12-dimethylbenz(*a*)anthracene can be significant irritants, resulting in chronic inflammation, necrosis, sloughing of tissue, and the formation of organizing granulation tissue (41). The etiology, type of inflammatory cell infiltrate, and therefore perhaps mechanisms in this type of injurious situation are likely to be different from what one sees in the human condition. Furthermore, these factors make it difficult to study premalignant lesions because inflammation itself can cause cytologic and/or morphologic changes that can be confused with dysplasia. Because 4-NQO treatment does not result in this type of injurious nonspecific inflammation, it is more likely to reflect the events that occur during human HNSCC.

Although 4-NQO has been used as a carcinogenic agent to induce tumors in animal models since the 1950s, and in the oral cavity since the 1970s (42, 43), a thorough review of the literature failed to reveal studies that were specifically designed to characterize the histopathologic changes that develop over time in the 4-NQO mouse model. Furthermore, the route of administration, the amount of carcinogen used, and the duration of treatment schedules have been highly variable. Therefore, we sought to characterize the optimal dosage and timing of 4-NQO treatment and to establish a timeline for the reproducible development of lesions showing hyperkeratosis, dysplasia, and HNSCC. Using two different doses and two different durations of treatment, we determined that 100 μg/mL in the drinking water for 8 weeks provided the most preferable results. This decision was based on the fact that this treatment protocol resulted in the development of singular or occasionally synchronous oral lesions. This aspect was critical because we wanted to refine the model to ensure that the mice developed lesions in a fashion that was most similar to the human condition rather than forming innumerable ones. In addition, the prescribed dosage and timing of treatment resulted in a predictable histologic progression over the 24-week period of time. Specifically, the data show that after the completion of carcinogen treatment, the predominant histopathologic diagnoses are hyperkeratosis at weeks 4 and 8, dysplasia at weeks 12, 14, and 16, and HNSCC at week 24 (Fig. 3). Importantly, the establishment of the progression timeline in this model will allow for future studies aimed at investigating the molecular and biological alterations that occur during the premalignant phase of HNSCC as well as for the validation of potential diagnostic biomarkers.

The induction of new blood vessel growth is a critical tumor phenotype in all malignancies, including HNSCC. There is considerable interest in determining how cells, progressing from normal to tumorigenic, make this switch. In some animal models, a distinct switch to the angiogenic phenotype is seen (44). In other cases, the cells developing into tumors sequentially become more angiogenic in a stepwise fashion (8, 45). Although the phenotype has been studied using animal models as well as human cells and tissue, the mechanisms about how this occurs in HNSCC are unknown. However, although the phenotypic changes in these models are similar to the human condition, the specific mechanisms involved in the induction of new blood vessel growth can be quite different. For example, although the major angiogenic factor in the hamster buccal pouch model is transforming growth factor-β (8), this growth factor has not been found to be a significant participant in the induction of angiogenesis in human HNSCC. Rather, a different subset of growth factors, including interleukin-8 and VEGF, seems to play predominant roles (35). As there were no data about the angiogenic phenotype in the 4-NQO mouse model, we sought to determine the timing of the

Published OnlineFirst March 31, 2009; DOI: 10.1158/1940-6207.CAPR-08-0211

appearance of this phenotype as well as identify the angiogenic factors that might be involved. The determination of MVD in tissue sections, using endothelial cell markers such as factor VIII, CD31, and/or CD34, is an accepted surrogate marker for *in vivo* angiogenesis. In the 4-NQO–treated animals, we observed a statistically significant increase in MVD as early as the hyperkeratotic stage, thereby showing that, much like other models as well as the human condition, the expression of the angiogenic phenotype is an early phenotypic change (Fig. 6). Furthermore, we observed sequentially increasing levels of VEGF expression at the stages of hyperkeratosis, dysplasia, and HNSCC (Fig. 6B and C). The mechanisms for this sequential increase are not known at this time. However, one could hypothesize that the progressive increase in VEGF expression might in part be the result of potential tumor-stroma paracrine interactions (46). The design of the study did not allow us to functionally validate whether VEGF was the key angiogenic factor produced in this animal model. However, the concordant increased expression of both MVD and VEGF supports the hypothesis that VEGF plays a central role in the expression of the angiogenic phenotype in the mouse 4-NQO model.

We have shown that daily treatment with ABT-510 for 24 weeks resulted in limited toxicity and significantly decreased the incidence of dysplasias and carcinomas in the mouse 4-NQO model of HNSCC (Fig. 3). The rationale for the 24-week treatment schedule was based on the observed cancer incidence and histologic diagnosis in our preliminary studies. As a result of these findings, animals were subsequently sacrificed at the same regular intervals over the 24-week time course to synchronize the treatment arm results with the initial histologic observations. Specifically, we observed most HNSCC (72%) at week 24, whereas dysplasia was the predominant histologic diagnosis at weeks 16 (55%) and 20 (60%). Because we were testing the hypothesis that ABT-510 would reduce the incidence of HNSCC, we believe it was most appropriate to carry out the prevention study to a time point where the predominant histologic diagnosis in the control group would be expected to be HNSCC. Overall, we observed a 46% cumulative reduction in the incidence of HNSCC between the control and treatment groups (37.3% versus 20.3%; $P = 0.021$). We did observe a small increase of HNSCC in the treatment group at week 20 when compared with the 20-week control group. However, this difference was not statistically significant ($P = 0.273$). The reasons for this observation are unknown but may be the result of uneven cohort sizes between the control and treatment groups within and at different sacrifice points. For example, the week 20 treatment group contained fewer animals ($n = 16$) than some of the other time points, such as week 24 ($n = 21$). The differences in cohort sizes at the given time points were a reflection of the fact that our initial experiments determined that week 24 should be the major cancer end point of this study. As such, although we were interested in synchronizing the treatment arm results with the histologic studies, we also felt it was most important to have the largest "n" at the major end point of the study. Further, it should be noted that the 16- and 24-week time points showed significant differences in the incidence of HNSCC between the control and treatment groups. For example, at 24 weeks, the difference in HNSCC incidence between the control and treatment groups was 72% versus 29%, respectively ($P = 0.007$). Finally, we also observed a cumulative decrease of 39% in the incidence of both dysplasia and HNSCC between the control and ABT-510 treatment groups (82.7% versus 50.6%; $P < 0.001$), the rates being higher in the control groups at each time point except for week 4 where there was only one case of dysplasia. Overall, these cumulative data strongly support the contention that ABT-510 was effective at decreasing the incidence of dysplasia and HNSCC in the mouse 4-NQO model of oral carcinogenesis.

The integration of inhibitors of angiogenesis into the treatment regimens of various diseases is increasing in frequency (47, 48). However, although there has been considerable discussion about the potential role of antiangiogenic agents in the area of chemoprevention, there are limited data to support the role of this class of drugs in this clinical setting (49, 50). ABT-510 is a mimetic peptide of thrombospondin-1 and acts as an inhibitor of angiogenesis by modulating the ability of endothelial cells to respond to various angiogenic factors. Specifically, ABT-510 binds to CD36, thereby inducing caspase-8–mediated endothelial cell apoptosis. This mechanism has been shown to block angiogenesis *in vitro* and *in vivo* as well as slow tumor growth in preclinical studies (24–29). Further, it has been tested clinically for the treatment of inflammatory bowel disease and in cancer therapy as a single agent or in combination with chemotherapeutic agents (51–55). Because it directly abrogates the ability of endothelial cells to respond to angiogenic factors, rather than altering the expression of these factors by tumor and/or stromal cells, one does not typically observe the direct modulation of various angiogenic factors in tumor cells. In keeping with these previous observations, we did not observe an alteration in the expression of VEGF by the oral keratinocytes in the treatment group animals (data not shown). However, the nearly 2-fold decrease in the incidence of HNSCC in the ABT-510 group at 24 weeks shows that the drug has a potent effect *in vivo* in this animal model.

One of the long-term goals of chemoprevention must be the development of treatments that can be easily taken by at-risk individuals for prolonged periods of time with minimal side affects to achieve widespread acceptance and long-term compliance. This would be particularly important in the case of high-risk patients who have not yet developed their first malignancy. As such, because ABT-510 is not an orally administered agent, it is unlikely that it would be found acceptable in its current form. Nonetheless, our proof-of-principle findings support the hypothesis that inhibitors of angiogenesis may have activity as chemopreventive agents. Furthermore, many of the chemopreventive agents currently under investigation, such as epidermal growth factor receptor tyrosine kinase inhibitors and cyclooxygenase-2 inhibitors, have multiple activities, including the inhibition of angiogenesis. However, the toxicities observed at the current prescribed dosages may preclude them from being used widely as chemopreventive agents. Therefore, the combination of one or both of these agents at lower doses in concert with other antiangiogenic agents may reduce toxicities and improve efficacy. The data presented here show proof of principle that the induction of new blood vessel growth by premalignant cells may be one such phenotype that could be targeted in a "chemoprevention cocktail."

Disclosure of Potential Conflicts of Interest

No potential conflicts of interest were disclosed.

Published OnlineFirst March 31, 2009; DOI: 10.1158/1940-6207.CAPR-08-0211

References

1. Jemal A, Siegel R, Ward E, et al. Cancer statistics, 2008. CA Cancer J Clin 2008;58:71–96.

2. Murphy GP, Lenhhardt LW. American Cancer Society textbook of clinical oncology. 2nd ed. Atlanta: American Cancer Society; 1995.

3. Day GL, Blot WJ. Second primary tumors in patients with oral cancer. Cancer 1992;70:14–9.

4. Slaughter DP, Southwick HW, Smejkal W. Field cancerization in oral stratified squamous epithelium; clinical implications of multicentric origin. Cancer 1953;6:963–8.

5. Lippman SM, Hong WK. Second malignant tumors in head and neck squamous cell carcinoma: the overshadowing threat for patients with early-stage disease. Int J Radiat Oncol Biol Phys 1989; 17:691–4.

6. Kelloff GJ, Lippman SM, Dannenberg AJ, et al. Progress in chemoprevention drug development: the promise of molecular biomarkers for prevention of intraepithelial neoplasia and cancer—a plan to move forward. Clin Cancer Res 2006;12:3661–97.

7. Carmeliet P. Angiogenesis in life, disease and medicine. Nature 2005;438:932–6.

8. Lingen MW, DiPietro LA, Solt DB, Bouck NP, Polverini PJ. The angiogenic switch in hamster buccal pouch keratinocytes is dependent on TGFβ-1 and is unaffected by ras activation. Carcinogenesis 1997;18:329–38.

9. Carlile J, Harada K, Baillie R, et al. Vascular endothelial growth factor (VEGF) expression in oral tissues: possible relevance to angiogenesis, tumour progression and field cancerisation. J Oral Pathol Med 2001;30:449–57.

10. Pazouki S, Chisholm DM, Adi MM, et al. The association between tumour progression and vascularity in the oral mucosa. J Pathol 1997;183:39–43.

11. Jin Y, Tipoe GL, White FH, Yang L. A quantitative investigation of immunocytochemically stained blood vessels in normal, benign, premalignant and malignant human oral cheek epithelium. Virchows Arch 1995;427:145–51.

12. Steidler NE, Reade PC. Experimental induction of oral squamous cell carcinomas in mice with 4-nitroquinolone-1-oxide. Oral Surg Oral Med Oral Pathol 1984;57:524–31.

13. Hawkins BL, Heniford BW, Ackermann DM, Leonberger M, Martinez SA, Hendler FJ. 4NQO carcinogenesis: a mouse model of oral cavity squamous cell carcinoma. Head Neck 1994;16:424–32.

14. von Pressentin MM, Kosinska W, Guttenplan JB. Mutagenesis induced by oral carcinogens in lacZ mouse (MutaMouse) tongue and other oral tissues. Carcinogenesis 1999;20:2167–70.

15. Thomas GR, Chen Z, Oechsli MN, Hendler FJ, Van Waes C. Decreased expression of CD80 is a marker for increased tumorigenicity in a new murine model of oral squamous-cell carcinoma. Int J Cancer 1999;82:377–84.

16. Kim TW, Chen Q, Shen X, et al. Oral mucosal carcinogenesis in SENCAR mice. Anticancer Res 2002;22:2733–40.

17. Tang XH, Knudsen B, Bemis D, Tickoo S, Gudas LJ. Oral cavity and esophageal carcinogenesis modeled in carcinogen-treated mice. Clin Cancer Res 2004;10:301–13.

18. Miyamoto S, Yasui Y, Kim M, et al. A novel rasH2 mouse carcinogenesis model that is highly susceptible to 4-NQO-induced tongue and esophageal carcinogenesis is useful for preclinical chemoprevention studies. Carcinogenesis 2008;29:418–26.

19. Brudno M, Poliakov A, Salamov A, et al. Automated whole-genome multiple alignment of rat, mouse, and human. Genome Res 2004;14:685–92.

20. Hancock JM. A bigger mouse? The rat genome unveiled. Bioessays 2004;26:1039–42.

21. Twigger SN, Shimoyama M, Bromberg S, Kwitek AE, Jacob HJ. The Rat Genome Database, update 2007—easing the path from disease to data and back again. Nucleic Acids Res 2007;35:D658–62.

22. O'Brien SJ, Menotti-Raymond M, Murphy WJ, et al. The promise of comparative genomics in mammals. Science 1999;286:458–62, 479–81.

23. Haviv F, Bradley MF, Kalvin DM, et al. Thrombospondin-1 mimetic peptide inhibitors of angiogenesis and tumor growth: design, synthesis, and optimization of pharmacokinetics and biological activities. J Med Chem 2005;48:2838–46.

24. Dawson DW, Volpert OV, Pearce SF, et al. Three distinct ›d-amino acid substitutions confer potent antiangiogenic activity on an inactive peptide derived from a thrombospondin-1 type 1 repeat. Mol Pharmacol 1999;55:332–8.

25. Anderson JC, Grammer JR, Wang W, et al. ABT-510, a modified type 1 repeat peptide of thrombospondin, inhibits malignant glioma growth *in vivo* by inhibiting angiogenesis. Cancer Biol Ther 2007;6: 454–62.

26. Yang Q, Tian Y, Liu S, et al. Thrombospondin-1 peptide ABT-510 combined with valproic acid is an effective antiangiogenesis strategy in neuroblastoma. Cancer Res 2007;67:1716–24.

27. Rusk A, McKeegan E, Haviv F, Majest S, Henkin J, Khanna C. Preclinical evaluation of antiangiogenic thrombospondin-1 peptide mimetics, ABT-526 and ABT-510, in companion dogs with naturally occurring cancers. Clin Cancer Res 2006;12: 7444–55.

28. Yap R, Veliceasa D, Emmenegger U, et al. Metronomic low-dose chemotherapy boosts CD95-dependent antiangiogenic effect of the thrombospondin peptide ABT-510: a complementation antiangiogenic strategy. Clin Cancer Res 2005;11:6678–85.

29. Reiher FK, Volpert OV, Jimenez B, et al. Inhibition of tumor growth by systemic treatment with thrombospondin-1 peptide mimetics. Int J Cancer 2002; 98:682–9.

30. Abbey LM, Kaugars GE, Gunsolley JC, et al. Intraexaminer and interexaminer reliability in the diagnosis of oral epithelial dysplasia. Oral Surg Oral Med Oral Pathol Oral Radiol Endod 1995;80:188–91.

31. Warnakulasuriya S, Reibel J, Bouquot J, Dabelsteen E. Oral epithelial dysplasia classification systems: predictive value, utility, weaknesses and scope for improvement. J Oral Pathol Med 2008; 37:127–33.

32. Hasina R, Whipple ME, Martin LE, Kuo WP, Ohno-Machado L, Lingen MW. Angiogenic heterogeneity in head and neck squamous cell carcinoma: biological and therapeutic implications. Lab Invest 2008;88:342–53.

33. Hasina R, Pontier AL, Fekete MJ, et al. NOL7 is a nucleolar candidate tumor suppressor gene in cervical cancer that modulates the angiogenic phenotype. Oncogene 2006;25:588–98.

34. Cuzick J. A Wilcoxon-type test for trend. Stat Med 1985;4:87–90.

35. Lingen MW. Angiogenesis in the development of head and neck cancer and its inhibition by chemopreventive agents. Crit Rev Oral Biol Med 1999;10: 153–64.

36. Heniford BW, Shum-Siu A, Leonberger M, Hendler FJ. Variation in cellular EGF receptor mRNA expression demonstrated by *in situ* reverse transcriptase polymerase chain reaction. Nucleic Acids Res 1993;21:3159–66.

37. Takeuchi S, Nakanishi H, Yoshida K, et al. Isolation of differentiated squamous and undifferentiated spindle carcinoma cell lines with differing metastatic potential from a 4-nitroquinoline N-oxide-induced tongue carcinoma in a F344 rat. Jpn J Cancer Res 2000;91:1211–21.

38. Yuan B, Heniford BW, Ackermann DM, Hawkins BL, Hendler FJ. Harvey ras (H-ras) point mutations are induced by 4-nitroquinoline-1-oxide in murine oral squamous epithelia, while squamous cell carcinomas and loss of heterozygosity occur without additional exposure. Cancer Res 1994;54:5310–7.

39. Chang SE, Bhatia P, Johnson NW, et al. Ras mutations in United Kingdom examples of oral malignancies are infrequent. Int J Cancer 1991; 48:409–12.

40. Homberger F. Chemical carcinogenesis in Syrian hamsters. Prog Exp Tumor Res 1972;16:152–75.

41. Eveson JW, MacDonald DG. Quantitative histological changes during early experimental carcinogenesis in the hamster cheek pouch. Br J Dermatol 1978;98:639–44.

42. Vered M, Yarom N, Dayan D. 4NQO oral carcinogenesis: animal models, molecular markers and future expectations. Oral Oncol 2005;41:337–9.

43. Kanojia D, Vaidya MM. 4-Nitroquinoline-1-oxide induced experimental oral carcinogenesis. Oral Oncol 2006;42:655–67.

44. Folkman J, Hanahan D. Princess Takamatsu Symposium. 1991, p. 339–47.

45. Volpert OV, Dameron KM, Bouck N. Sequential development of an angiogenic phenotype by human fibroblasts progressing to tumorigenicity. Oncogene 1997;14:1495–502.

46. Liss C, Fekete MJ, Hasina R, Lam CD, Lingen MW. Paracrine angiogenic loop between head-and-neck squamous-cell carcinomas and macrophages. Int J Cancer 2001;93:781–5.

47. Ferrara N, Kerbel RS. Angiogenesis as a therapeutic target. Nature 2005;438:967–74.

48. Kerbel R, Folkman J. Clinical translation of angiogenesis inhibitors. Nat Rev Cancer 2002;2:727–39.

49. Albini A, Noonan DM, Ferrari N. Molecular pathways for cancer angioprevention. Clin Cancer Res 2007;13:4320–5.

50. Sharma RA, Harris AL, Dalgleish AG, Steward WP, O'Byrne KJ. Angiogenesis as a biomarker and target in cancer chemoprevention. Lancet Oncol 2001;2:726–32.

51. Ebbinghaus S, Hussain M, Tannir N, et al. Phase 2 study of ABT-510 in patients with previously untreated advanced renal cell carcinoma. Clin Cancer Res 2007;13:6689–95.

52. Markovic SN, Suman VJ, Rao RA, et al. A phase II study of ABT-510 (thrombospondin-1 analog) for the treatment of metastatic melanoma. Am J Clin Oncol 2007;30:303–9.

53. Gietema JA, Hoekstra R, de Vos FY, et al. A phase I study assessing the safety and pharmacokinetics of the thrombospondin-1-mimetic angiogenesis inhibitor ABT-510 with gemcitabine and cisplatin in patients with solid tumors. Ann Oncol 2006;17:1320–7.

54. Hoekstra R, de Vos FY, Eskens FA, et al. Phase I study of the thrombospondin-1-mimetic angiogenesis inhibitor ABT-510 with 5-fluorouracil and leucovorin: a safe combination. Eur J Cancer 2006; 42:467–72.

55. Hoekstra R, de Vos FY, Eskens FA, et al. Phase I safety, pharmacokinetic, and pharmacodynamic study of the thrombospondin-1-mimetic angiogenesis inhibitor ABT-510 in patients with advanced cancer. J Clin Oncol 2005;23:5188–97.

AACR American Association for Cancer Research

Cancer Prevention Research

ABT-510 Is an Effective Chemopreventive Agent in the Mouse 4-Nitroquinoline 1-Oxide Model of Oral Carcinogenesis

Rifat Hasina, Leslie E. Martin, Kristen Kasza, et al.

Cancer Prev Res 2009;2:385-393. Published OnlineFirst March 31, 2009.